Available online at www.sciencedirect.com
ScienceDirect
International Journal of Pharmaceutics 344 (2007) 143–149
INTERNATIONAL JOURNAL OF PHARMACEUTICS
www.elsevier.com/locate/ijpharm

In vivo evaluation of lipid nanocapsules as a promising colloidal carrier for paclitaxel

F. Lacoeuille [a,b,*], F. Hindre [a,b], F. Moal [c], J. Roux [d], C. Passirani [a,b], O. Couturier [a,b], P. Cales [c], J.J. Le Jeune [a,b], A. Lamprecht [e], J.P. Benoit [a,b]

[a] *Inserm U646, 10 rue A. Boquel, F-49100 Angers, France*
[b] *University of Angers, 10 rue A. Boquel, F-49100 Angers, France*
[c] *Laboratory HIFI, UPRESS EA3589, University of Angers, F-49100 Angers, France*
[d] *SCAHU, UFR Medecine, University of Angers, F-49100 Angers, France*
[e] *Laboratory of Pharmaceutical Engineering, Faculty of Medicine and Pharmacy, University of Franche-Comté, Place Saint Jacques, F-25030 Besançon, France*

Received 15 February 2007; received in revised form 8 June 2007; accepted 13 June 2007
Available online 19 June 2007

Abstract

Paclitaxel-loaded lipid nanocapsules (PX-LNC) exhibit interesting *in vitro* characteristics with improved antitumoral activity compared with free PX formulation. Biodistribution studies were realized with the use of ^{14}C-trimyristin (^{14}C-TM) or ^{14}C-phosphatidylcholine (^{14}C-PC) whereas antitumoral activity of PX-LNC formulations was based on the animal survival in a chemically induced hepatocellular carcinoma (HCC) model in Wistar rats. Blood concentration–time profiles for both labeled ^{14}C-TM-LNC and ^{14}C-PC-LNC were similar; the $t_{1/2}$ and MRT values (over 2 h and close to 3 h, respectively, for both formulations) indicated the long circulating properties of the LNC carrier with a slow distribution and elimination phase. Survival curves of paclitaxel treated groups showed a statistical significant difference compared to the control survival curve ($P = 0.0036$ and 0.0408). Animals treated with $4\times$ 70 mg/m^2 of PX-LNC showed the most significant increase in mean survival times compared to the controls (IST_{mean} 72%) and cases of long-term survivors were preferentially observed in the PX-LNC treated group (37.5%; 3/8). These results demonstrate the great interest to use LNC as drug delivery system for paclitaxel, permitting with an equivalent therapeutic efficiency to avoid the use of excipients such as polyoxyethylated castor oil for its formulation.

Keywords: Lipid nanocapsules; Drug delivery system; Biodistribution; Hepatocellular carcinoma; Paclitaxel

1. Introduction

Paclitaxel is a natural diterpenoid derivative and a major antineoplastic agent which shows a widespread antitumoral activity on various tumor cell lines thanks to its action on microtubules. According to its hydrophobicity and thus to its low water solubility, pharmaceutical excipients such as polyoxyethylated castor oil (Cremophor® EL) and ethanol are required to formulate parenteral solutions, with the main drawback for being responsible of major adverse effects such as hypersensitivity reactions (Gelderblom et al., 2001). Among the different strategies used to avoid such excipients, the development of nanocarriers (mainly liposome and nanoparticles), has been considered, for the past decades, as one of the most promising ways (Kawashima, 2001). Such nanocarrier-based formulations lead theoretically, to an increased drug solubility but also to a modified distribution, inducing, therefore, a higher therapeutic index. This strategy has already given some results, especially by limiting the adverse toxic effects of antineoplastic drugs (Sells et al., 1987), however, after intravenous administration, colloidal carriers were rapidly captured by the mononuclear phagocyte system (MPS) (Storm et al., 1987). This phenomenon, by limiting the circulation of the carrier, reduces their ability to distribute the drug towards its site of action, then, limiting its therapeutic effect. This issue has been overcome by modifying the surface of nanocarriers and a major advance was realized when, by coating the surface of conventional particles with hydrophilic polymers, such

* Corresponding author at: University of Angers, 10 rue A. Boquel, F-49100 Angers, France. Tel.: +33 2 41 73 58 55; fax: +33 2 41 73 58 53.
E-mail address: franck.lacoeuille@univ-angers.fr (F. Lacoeuille).

0378-5173/$ – see front matter © 2007 Elsevier B.V. All rights reserved.
doi:10.1016/j.ijpharm.2007.06.014

as polyoxyethylene, it has been possible to reduce opsonization and subsequent elimination by the MPS (Torchilin and Trubetskoy, 1995). This strategy led to prolonged blood circulation time of the carriers, so-called "stealth™" carriers are able, due to the tumor defective vascular architecture and impaired lymphatic clearance, to accumulate in tumor tissue and enhance pharmacological efficacy of the encapsulated drug (Moghimi et al., 2001). This concept for the tumor selective drug targeting by macromolecules or nanoparticles is known as the enhanced permeability and retention effect (EPR) (Maeda et al., 2000).

The recently described phase inversion process allowed the preparation of lipid nanocapsules (LNC) in a size range between 25 to around 110 nm without the use of organic solvents (Heurtault et al., 2002). We previously reported our ability to entrap high drug loading of paclitaxel into LNC (PX-LNC) and demonstrated sustained drug release properties (Lacoeuille et al., in press). Preliminary studies in cell culture demonstrated a higher efficiency of PX-LNC in cancer cell death induction compared to commercial formulation and the next step, presented here, was to perform our *in vivo* evaluation of the carrier in the objective to assess, comparatively to free paclitaxel, the therapeutic equivalency of this innovative drug delivery system for paclitaxel. For the blood and tissue distribution studies we used ^{14}C-labeled LNC formulations based on the use of ^{14}C-lipids (phosphatidylcholine and trimyristin) as markers of LNC, whereas antitumoral activity of paclitaxel-loaded LNC was based on the mean survival time in tumor-bearing rats. The chemically induced hepatocellular carcinoma (HCC) tumor model was chosen for several reasons. HCC is considered as one of the most common cancers in the world and the first primary malignant tumor of liver (Seeff, 2004). Until now, different therapy modalities have been under investigation, mostly with disappointing results. Curative therapy is rarely achieved except when surgical treatments (ablative treatment or hepatic transplantation) are feasible (Clark et al., 2005). Systemic monochemotherapy leads to low response rate without survival improvement whereas polychemotherapy could achieve complete response but, due to its toxicity, only on selected patients possessing relatively good hepatic function (Forner et al., 2006). HCC is also known to be chemoresistant to anticancer drugs by overexpressing the multidrug resistant (MDR) mdr1 gene and its product, the P-glycoprotein (Ng et al., 2000). P-glycoprotein limits accumulation of lipophilic and cationic drugs into tumor cells by increasing their efflux, leading to the tumor cells' resistance to chemotherapeutics agents. LNC-based chemotherapy could be an interesting alternative to classical formulations in this pathology, especially, because they have demonstrated to inhibit P-glycoprotein related transporting systems (Lamprecht and Benoit, 2006) which contribute to the MDR phenomenon. In this work, we studied therapeutic efficiency of paclitaxel-loaded LNC on the HCC model versus classical formulation of paclitaxel and controls.

2. Materials and methods

2.1. Materials

Paclitaxel was purchased from Indena SpA (Milan, Italy), neutral oil (Labrafac® CC), was a kind gift from Gattefosse (Saint-Priest, France). Lipoïd® S75-3 (Soybean lecithin) and Solutol® HS15 (a mixture of polyethylene glycol-660 hydroxystearate (PEG-HS) and free polyethylene glycol chains) were kind gifts from Lipoid GmbH (Ludwigshafen, Germany) and BASF AG (Ludwigshafen, Germany), respectively. NaCl was obtained from VWR international (Fontenay-sous-Bois, France) and water from a Milli RO System (Millipore, Paris, France). Radiolabeled trimyristin (myristic-1-^{14}C) and phosphatidylcholine (dipalmitoyl-1-^{14}C) were purchased from Isobio (Fleurus, Belgium).

2.2. Nanocapsules preparation

Preparation of PX-LNC was based on the phase inversion process previously described (Heurtault et al., 2003; Lacoeuille et al., in press). First, paclitaxel (20 mg) was solubilized into 514 mg of the neutral oil phase (i.e. Labrafac®) to achieve entrapment into the LNC core. Thereafter, all components (see Table 1 for relative proportions of the LNC components) were mixed and heated under magnetic stirring up to 85 °C in order to ensure to pass the phase inversion temperature. The following cooling step was performed until an exact temperature of 55 °C passing the phase inversion zone completely again. This cycle was repeated

Table 1
Physico-chemical characteristics of LNC constituents and nanocapsules

	Labrafac®	Solutol® HS15		Lipoïd®		NaCl	Water
		PEG (30%)	PEG-HS (70%)	PE (10%)	PC (70%)		
Relative proportions	20.6	16.9		1.5		1.8	59.2
Molecular weight (g mol^{-1})	470	660	960	740	780	–	–
Density (g mL^{-1})	0.946	1	1	0.97	0.97	–	–
Radius of the LNC core, r_{core} (nm)	20.74			–			
Surface of the LNC core, S_{core} (m^2 mL^{-1})	9.09			–			
Radius of the LNC shell, r_{shell} (nm)	–		4.66			–	–
Surface of the LNC shell, S_{shell} (m^2 mL^{-1})	–		13.63			–	–
Surface density (molecules/nm^2)	–	1.45	2.33	0.034	0.227	–	–
Surface area (nm^2 per molecule)	–	0.69	0.43	29.41	4.40	–	–
Distance between two molecules (nm)	–	0.83	0.65	5.42	2.10	–	–

Table 2
Characteristics of ^{14}C-PC-LNC labeled with phosphatidylcholine (dipalmitoyl-1-^{14}C) and ^{14}C-TM-LNC labeled with trimyristin (myristic-1-^{14}C)

	Size (nm)	Polydispersity index	Specific activity (MBq/mL)	Activity recovery (%)	Labeling yield (%)
^{14}C-PC-LNC	54.7 ± 0.1	0.051 ± 0.037	0.073	95.26	97.51
^{14}C-TM-LNC	55.6 ± 0.8	0.048 ± 0.033	0.016	96.68	97.89

another two times before adding 2.5 mL of distilled water at 2 °C to obtain 5 mL of the final PX-LNC suspension. For the radiolabeling procedure ^{14}C-labeled lipids were mixed to the internal neutral oily phase of the LNC. Two kinds of formulation were obtained: ^{14}C-TM-LNC were labeled with ^{14}C-trimyristin and ^{14}C-PC-LNC with ^{14}C-phosphatidylcholine. The respective proportions of constituents (Table 1) were chosen in order to obtain particles with a diameter size around 50 nm (Table 2). Paclitaxel was also formulated, like the commercial formulation, in a mixture of ethanol and polyoxyethylated castor oil (Cremophor EL) (50/50 v/v), this formulation was called the free paclitaxel formulation and was used to compare with PX-LNC group in the survival studies.

2.3. Characterization of LNC formulations

Size measurements consisting of mean diameter and polydispersity index were determined by PCS using a Malvern Autosizer 4700 (Malvern instruments S.A., Worcestershire, United Kingdom) fitted with a 488 nm laser beam at fixed angle (90°) at 25 °C. All batches were diluted with distilled water prior to the analysis and each measurement was performed in triplicate. PEG and HS-PEG densities (i.e. Solutol® HS 15 density), surface area occupied by one molecule and distance between molecules at the surface of LNC were determined as previously described (Vittaz et al., 1996) using PCS size measurements and the relative proportions of each LNC constituent (Table 1). In fact, theoretical volume of a single nanocapsule was calculated using mean diameter measurements ($V = 4/3\pi r^3$). Considering all constituents incorporated into the nanocapsules formulation, total volume of all nanocapsules (V_T) was calculated by addition of each LNC constituent's volume. The total number (n) of nanocapsules was deduced from previous calculations ($n = V_T/V$) and divided by the volume of the LNC suspension (V_S, varying from 5 to 17 mL according to the formulation) to obtain a number of nanocapsules per milliliter. Labrafac® volume used for one formulation and the total number of nanocapsules estimated led to the volume of the core (V_{core}), the mean radius (r_{core}) and surface (S_{core}) of the LNC core ($S_{core} = 4\pi r_{core}^2$). The radius of the shell (r_{shell}) composed by Solutol® and Lipoïd® was deduced from the difference $(r) - (r_{core})$. All this parameters led us to the determination of PEG and HS-PEG densities. Radioactivity measurements were realized by adding 5 mL of a scintillation solution (Ultima-Gold®, Packard Bioscience B.V., Groningen, The Netherlands) to LNC suspension (1 mL). Each sample was counted with a beta scintillation counter (Tri-Carb-2300TR, Packard Instrument Company, Meriden, USA) three times during 10 min. The activity recovery of the LNC suspension was determined according to Eq. (1) whereas percentage of incorporation of ^{14}C-labeled lipids into LNC was determined by dialysis studies. ^{14}C-TM-LNC were dialyzed under magnetic stirring for 48 h against distilled water. After that time, dialysate samples (1 mL) were collected into scintillation vials and counted for the determination of a labeling yield as shown in Eq. (2). The *in vitro* stability of the LNC labeling was expressed as the labeling yield variation versus the dialysis time:

$$\text{Activity recovery}\,(\%) = \frac{\text{measured LNC activity}}{\text{theoretical LNC activity}} \times 100 \quad (1)$$

$$\text{Labeling yield}\,(\%) = \frac{\text{activity of LNC after dialysis}}{\text{activity of LNC before dialysis}} \times 100 \quad (2)$$

2.4. In vivo studies

For *in vivo* studies Wistar rats were obtained from the animal house of the Angers University Hospital. The animals were kept in standard animal facilities with two rats per cage and given free access to food and water. They were housed in a temperature and humidity controlled room with 12 h on–off light cycles and euthanized at the end of each experiment.

2.4.1. Biodistribution studies

Blood distribution studies were realized with 13 Wistar rats (320–450 g), divided in two groups, one injected with ^{14}C-PC-LNC ($n = 8$) and the other with ^{14}C-TM-LNC ($n = 5$). Prior to experiments, catheterisation and tunnelling of the femoral vein were performed to allow subsequent numerous blood sampling. Experiments started with intravenous injection of ^{14}C-labeled LNC suspension (1 mL) to rats via penis vein. At the indicated time intervals 5, 10, 15, 30, 45, 60, 120, 180, 360, 540 and 720 min post-injection, blood samples (100 μL) were collected via the femoral vein catheter under isoflurane anaesthesia. Collected blood samples were dissolved in scintillation vials with 500 μL of Solvable® (Packard Bioscience B.V., Groningen, The Netherlands) during 4 h in a 60 °C bath. Samples were decolorized with 100 μL of EDTA (0.1 M) and 200 μL of a 30% hydrogen peroxide solution (Sigma–Aldrich, Saint Quentin Fallavier, France). After 1 h in a 50 °C bath, vials were added with 5 mL of the scintillation solution and counted. For tissue distribution studies, 24 rats (270–330 g) were divided in two groups ($n = 12$) injected with ^{14}C-PC-LNC and ^{14}C-TM-LNC, respectively. In both groups, animals were sacrificed at interval times of 1 h ($n = 6$) and 2 h ($n = 6$) post-injection, organs were removed, washed and weighted (liver, spleen, kidneys, heart, lungs, stomach and intestines). Tissue samples (50 μg) were

processed as for blood samples without EDTA and adding only 100 μL of a 30% hydrogen peroxide solution.

2.4.2. Pharmacokinetic analysis

To compare ^{14}C-PC-LNC and ^{14}C-TM-LNC suspensions, pharmacokinetic parameters such as total area under the curve (AUC_{tot}), half life ($t_{1/2}$), mean residence time (MRT) and clearance (Cl), were calculated using a non-compartmental model for analysis of pharmacokinetics data (Kinetica® v4.2 software, Innaphase, Philadelphia, PA, USA). In this model, AUC_{tot} was determined using the trapezoidal method during experimental period ($AUC_{[0\rightarrow 12]}$) added with extrapolated area ($AUC_{[t\rightarrow\infty]}$) calculated by dividing the last experimental concentration (C_t) by the elimination rate constant (K). MRT was expressed as the ratio of the total area under the first moment curve (AUMC) on AUC_{tot}.

All pharmacokinetics data were expressed as mean value and concentration in each organ as a mean value ± S.D. The non-parametric statistical test of Mann and Whitney was used with the Stat View Software version 5.0 (SAS Institute Inc.). The test was considered as significant when the P values were <0.05.

2.4.3. HCC model and treatment methodology

HCC model was chemically induced to 35 rats Wistar (145–226 g) by adding diethyl nitrosamine (DEN; $C_4H_{10}N_2O$) to drinking water (100 mg/L) during 10 weeks. Animals were randomized into four treatment groups. Each animal underwent four intravenous injections (one injection per week) during 4 weeks. Control group received saline injections ($n = 11$), control LNC group received blank-LNC injections ($n = 8$), control paclitaxel group ($n = 8$) was treated with injections of a free paclitaxel solution (70 mg/m^2) and at last LNC paclitaxel group ($n = 8$) was treated with intravenous injections of PX-LNC (70 mg/m^2).

2.4.4. Treatment efficiency

For the survival studies, origin point was fixed at the last day of tumor induction (i.e. 10 weeks after the beginning of tumor induction by DEN) and end point was determined by the death of the animal or a loss of weight during 3 weeks consecutively. To estimate treatment efficiency survival data were analyzed by the Kaplan–Meier method, using the Log-rank test (Mantel–Cox test). Stat View Software version 5.0 (SAS Institute Inc.) was used in that purpose and tests were considered as significant when the P values were <0.05. The four groups of treatment were also compared in term of estimated median survival time, increase in median survival time (IST_{median} %), mean survival time, increase in mean survival time (IST_{mean} %), long-term survivor (i.e. animal with a survival time two times higher than the median survival time of animals in the control saline group) and maximal survival time.

3. Results and discussion

3.1. Characterization of LNC formulations

Hydrodynamic diameter size measurements (mean diameter = 50.8 ± 0.1 nm) allowed us to determine physical characteristics such as volume (68.64×10^3 nm^3) and radius (25.4 nm) of the LNC. Calculus of average Solutol® HS-15 and Lipoïd® densities, surface area occupied by one molecule and distance between molecules at the surface of the core of Labrafac® for LNC are presented in Table 1. As it will be discussed for *in vivo* biodistribution results, a high Solutol® HS-15 density was observed on LNC surface with a majority of HS-PEG moieties versus PEG (2.33 molecules/nm^2 versus 1.45 molecules/nm^2), leading to a small intermolecular distance from 0.65 nm between HS-PEG chains up to 0.83 nm between PEG chains. Physico-chemical characterization of labeled-LNC, including size measurement and specific activity, percentage of radioactivity recovery and labeling yield determination are summarized in Table 2. The mean diameter of the LNCs was around 50 nm, with a polydispersity index always less than 0.1 showing the monodispersity of the preparation and that no size modification could be attributed to the labeling process. Activity recovery and labeling yield results (always more than 95%) showed that ^{14}C-labeled lipids were both incorporated with good yield into the LNC. Release of ^{14}C-trimyristin from ^{14}C-TM-LNC during dialysis studies was very slow (Fig. 1) with a maximum release lower than 2% after 48 h. Results clearly indicated that the use of ^{14}C-lipids did not alter the LNC structure and was a good strategy to follow *in vivo* behaviour of the carrier. In comparison, previous work on ^{125}I labeling showed an incorporation yield of only 20% with an increase of size (from 50 up to 65 nm) (Cahouet et al., 2002).

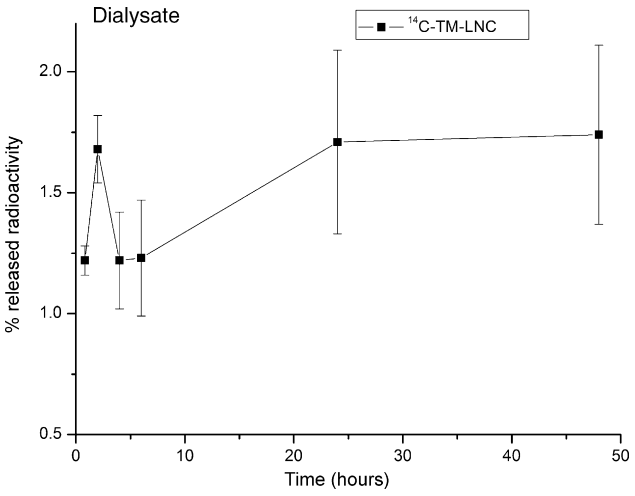

Fig. 1. Kinetics release of ^{14}C-trimyristin from ^{14}C-TM-LNC (■) during dialysis studies against distilled water for 48 h. The results are calculated as the ratio between radioactivity released in the dialysate and radioactivity incorporated in the ^{14}C-TM-LNC ($n = 3$).

3.2. Biodistribution studies

Blood concentration–time profiles for both labeled ^{14}C-TM-LNC and ^{14}C-PC-LNC preparations are shown in Fig. 2. The blood pharmacokinetics parameters obtained from labeled LNC are summarized in Table 3. The mean ^{14}C activity of both labeled LNC and control solution in various organs are presented in Fig. 3. After intravenous injection, ^{14}C activity slowly decreased

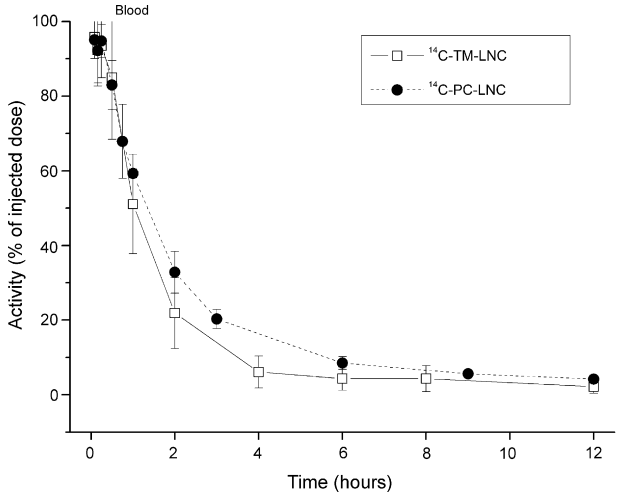

Fig. 2. Blood (^{14}C) concentration–time profiles of LNC labeled with ^{14}C-trimyristin (^{14}C-TM-LNC) ($n=5$) and labeled with ^{14}C-phosphatidylcholine (^{14}C-PC-LNC) ($n=8$) after intravenous injection in rats ($n=6$). Results are expressed as percent of injected dose.

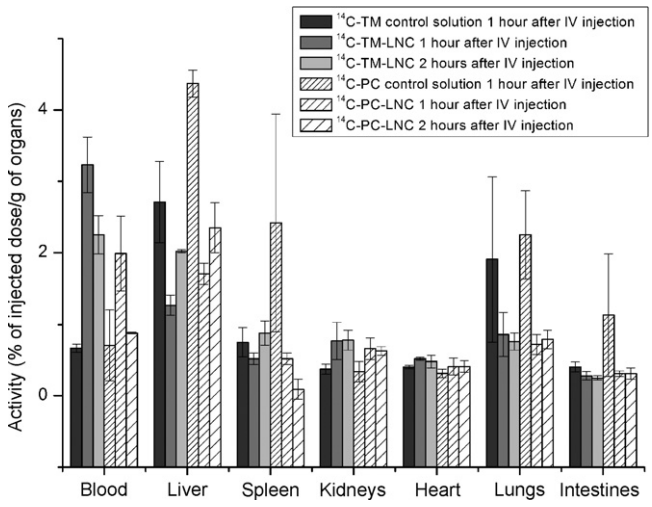

Fig. 3. Organs biodistribution of LNC labeled with ^{14}C-trimyristin (^{14}C-TM-LNC) ($n=5$), ^{14}C-trimyristin (^{14}C-TM) control solution ($n=2$), LNC labeled with ^{14}C-phosphatidylcholine ^{14}C-PC-LNC ($n=8$) and ^{14}C-PC control solution ($n=2$) 1 and 2 h after intravenous injection to rats. Results are expressed as a percent of injected dose per gram of organ.

from blood circulation as more than 50% of injected dose is still present 1 h post-injection. Both ^{14}C-TM-LNC and ^{14}C-PC-LNC preparations exhibited a similar clearance profile and no statistical difference was observed in the calculated pharmacokinetics parameters for both formulations ($P>0.05$). The $t_{1/2}$ and MRT values (over 2 h and close to 3 h, respectively, for both formulations) indicated the long circulating properties of the LNC carrier with a slow distribution and elimination phase. One and 2 h post-injection, labeled LNC and control solutions were compared by measuring the ^{14}C activity in various organs. Because of an increased liver and spleen uptake, about two times higher, a drastic difference was observed between ^{14}C-lipid markers control solutions, which are rapidly cleared from blood circulation, and labeled LNC. For labeled LNCs, ^{14}C activity disappearance from blood between the first and the second hour following injection was concomitant of its rise in MPS organs. These data underlined the major role of liver in LNC removal from blood circulation. On the opposite, other organs, such as kidneys, lungs and intestine kept a constant rate of ^{14}C during experiment. Biodistribution and pharmacokinetics of LNC were assessed using two different radioactive tracers; ^{14}C-trimyristin was used as a marker of LNC lipid core whereas ^{14}C-phosphatidylcholine was used as a marker of LNC shell. The use of ^{14}C-lipids labeling to characterize the *in vivo* LNC biodistribution profile was validated by *in vitro* study of LNC labeling stability and by following *in vivo* the fate of ^{14}C-lipid control solution. Blood distribution results were equivalent for both labeled LNCs and the stealth properties observed with this carrier were comparable with those achieved by other long circulating carriers such as surface-modified nanocapsules obtained from PLGA-PEG copolymers (Mosqueira et al., 2001). Despite the fact that PEG and HS-PEG chains present in LNC structure are very short (i.e. 0.660 and 0.960 kDa, respectively), when comparing pharmacokinetics data of LNC and PLA-PEG nanocapsules it is interesting to notice that we observed very similar results in terms of MRT, AUC and clearance especially with PLA-PEG nanocapsules with high contents (30%) and long (20 kDa) PEG chains (Mosqueira et al., 2001). These LNC stealth properties observed for very short PEG chains length could be explained by the presence of a comparatively higher density of PEG and HS-PEG chains on the LNCs surface (2.33 HS-PEG molecules/nm^2 and 1.45 PEG molecules/nm^2 for LNC versus 0.05 PEG molecules/nm^2 for PLA-PEG nanocapsules). Organs biodistribution results indicated that LNCs clearance from blood is mainly due to liver. This phenomenon could be explained by two classically described mechanisms. One is the action of Küpffer cells and other macrophages involved in the nanoparticles capture (Gibaud et al., 1996). The other hypothesized that the small size of LNC (50 nm) could facilitate their passage from blood to hepatocytes through the fenestrations (100 nm) of the sinusoidal endothelium of liver (Le Couteur et al., 2002).

Table 3
Blood pharmacokinetics parameters of both ^{14}C-TM-LNC ($n=5$) and ^{14}C-PC-LNC ($n=8$) after intravenous injection in rats

Blood PK parameters	^{14}C-TM-LNC	^{14}C-PC-LNC	*P* values
Dose (%)	100	100	–
AUC_{tot} (%dose min)	11217 ± 3420	13891 ± 2088	0.3055
$t_{1/2}$ (min)	143 ± 50	172 ± 77	0.6605
MRT (min)	159 ± 36	196 ± 57	0.2416
Cl (min^{-1})	0.0097 ± 0.0031	0.0073 ± 0.0010	0.3055

Table 4
Descriptive and statistical data from the survival study

Treatment group	*n*	Median	95% CI	IST_{median} (%)	Mean survival time	IST_{mean} (%)	Long-term survivors	Maximal survival time	*P* values
Control saline	11	53.0	35–82	–	54.2 ± 22.5	–	0	88	–
Blank LNC	8	57.0	49–74	8	62.9 ± 17.5	16	0	96	0.4082
Free PX solution	8	91.0	61–113	72	89.2 ± 31.4	65	2	133	0.0036
PX-LNC	8	76.0	63–140	43	93.4 ± 36.2	72	3	149	0.0408

Mean survival time is expressed as the mean value ± S.D. ($n = 8$). The increases in median survival time (IST_{median} %) and increases in the mean survival time (IST_{mean} %) are compared to control group. Survival data were analyzed using the Log-rank test (Mantel–Cox test) which was considered as significant when the *P* values were <0.05.

3.3. Survival study

The other goal of our study was to evaluate *in vivo* therapeutic efficiency of a new colloidal carrier for paclitaxel. The therapeutic scheme chosen for the survival studies was based, on a cycle of four cures of paclitaxel at the dose level of 70 mg/m^2, to mimic clinical practices. Because of a frequently faster elimination rate, dose regimen used for animals are often higher than for humans. In our case we used a lower dose of paclitaxel (i.e. 70 mg/m^2 versus 175 mg/m^2 in most clinical practice) due to volume limitation (1 mL) for intravenous injection to rats. Descriptive and statistical data from the survival study are presented in Table 4 and survival curves according to the Kaplan–Meier method are represented in Fig. 4. First of all, very similar results were found in the two control groups (i.e. control saline and blank-LNC groups), with only a slight increase of the median survival time (IST_{median} 8%) and mean survival time (IST_{mean} 16%) in the blank-LNC group and no statistical difference between the two survival curves ($P = 0.4082$; Table 4, Fig. 4). On the opposite, the two survival curves of paclitaxel treated groups showed a statistical significant difference with the control saline survival curve ($P = 0.0036$ and 0.0408; Table 4, Fig. 4). Animals treated with 4× 70 mg/m^2 of PX-LNC showed the most significant increase in mean survival times compared to the controls (IST_{mean} 72%), these results are close to those obtained with animals treated with 4× 70 mg/m^2 of free PX solution (IST_{mean} 65%). Moreover, cases of long-term survivors were preferentially observed in the PX-LNC treated group. Actually, none animals from control groups (0/11 + 0/8) survived after 106 days (two times the median of control saline group) whereas 25.0% (2/8) of the animals treated with a free PX solution (113 and 133 days; Fig. 4) and 37.5% (3/8) of those treated with PX-LNC were long-term survivors (116, 140 and 149 days; Fig. 4). In contrast, the increase of estimated median survival time is more pronounced in the free PX solution treated group (IST_{median} 72%) compared to results observed in the PX-LNC group (IST_{median} 43%). The confidence interval for estimated median results found in the control saline group (35–82 days), spread out in the PX treated groups to reach very wide intervals, 61–113 days in the free PX group and 63–140 days in the PX-LNC group, respectively, indicating clearly that some animals are low-responder and others high-responder to the treatment. Finally, during our survival study, we demonstrated the therapeutic efficiency of free PX solution and PX-LNC compared to controls in a model of HCC. Although that highest and mean survival times were found in the PX-LNC group there was no statistical difference with the survival curve of the free PX solution group, suggesting the therapeutic equivalency of both formulations.

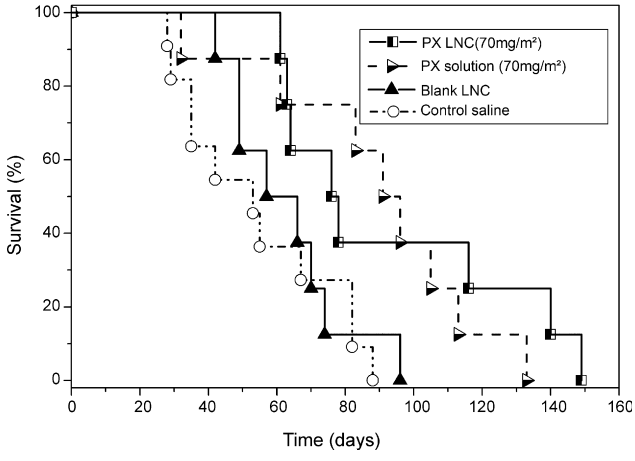

Fig. 4. Survival curves of 35 HCC tumor-bearing Wistar rats after various treatment (Kaplan–Meier plot). HCC was chemically induced by adding diethyl nitrosamine (DEN; $C_4H_{10}N_2O$) to animals' drinking water during 10 weeks. Wistar rats were then randomized into four groups of treatment. Treatment group consisted of free paclitaxel solution (▶ : 70 mg/m^2; $n = 8$), blank LNC (▲: $n = 8$), PX-LNC (◧ : 70 mg/m^2; $n = 8$) and control saline (◯; $n = 11$). Each animal received four intravenous injections via penis vein (one injection per week) during 4 weeks. For the survival studies origin point was fixed at the last day of treatment (i.e. 14 weeks after the beginning of tumor induction by DEN) and end point was determined by the death of the animal or a loss of weight during 3 weeks consecutively.

Several points can be discussed concerning survival results and the model of solid tumor used in this study. DEN-induced HCC is a classical animal model of liver carcinogenesis, widely used and described (Moal et al., 2001; Bralet et al., 2002; Faivre et al., 2004). The main advantage of this model consist of the fact that the liver carcinogenesis process observed in DEN model is based on a random clonal proliferation from mature hepatocytes and led to superimposable histological features as those observed with human HCC (Bralet et al., 2002). These characteristics are of interest to foresee future clinical application but are also challenging. Effectively, the main drawback of this type of model, as indicated in our study by the confidence interval for median time in the control saline group (Table 4), is the heterogeneous tumor growth process. Therefore, as shown in the two PX treated group, it is problematic to demonstrate a statistical efficiency difference between two

treatments, because long-term remissions are counterbalance by partial response in some animals whose liver carcinogenesis process is especially effective. Moreover, paclitaxel dose regimen used in this study ($4\times$ 70 mg/m^2), as evoked before, was chosen due to restrictive technical and animal facilities. If it has shown efficacy compared to controls, it can be optimized by the choice of more appropriate doses or new modalities for the treatment such as intra-arterial chemotherapy or transarterial chemoemboliazion (TACE) (Barone et al., 2003; Gerolami et al., 1998). In fact, the tumor selective drug targeting and well known concept of enhanced permeability and retention effect (EPR), could not be completely obtain after intravenous administration of chemotherapy, since HCC tumor blood supply is mainly dependent on hepatic artery (Breedis and Young, 1954). Liver carcinogenesis process is concomitant to structural changes in the vascularization whereby the normal fenestration of liver sinusoidal endothelial cells is abrogated leading to predominant arterial vascularization of the tumor (Gerolami et al., 1998). Our investigation was a first preliminary *in vivo* evaluation of a new colloidal carrier for paclitaxel. Previous work has shown the ability of ^{188}Re-labeled LNC to be promising radiotracers for radiotherapy (Ballot et al., 2006). With this study, PX-LNC exhibited relevant characteristics for HCC chemotherapy and authorize the use of LNC for future combined therapies, chemotherapy and internal radiotherapy, in association between PX-LNC and ^{188}Re-LNC.

4. Conclusion

In this work we demonstrated the long circulating properties of LNC and the therapeutic efficiency of PX-LNC compared to controls in a model of HCC. Survival studies in a HCC model concluded to the therapeutic equivalency of the paclitaxel-loaded nanocapsules comparatively with classical paclitaxel formulation. LNC exhibit the great advantage to avoid the use of Cremophor® EL for the solubilization and formulation of paclitaxel, PX-LNC are, therefore, proposed as new drug delivery system for paclitaxel.

References

Ballot, S., Noiret, N., Hindre, F., Denizot, B., Garin, E., Rajerison, H., Benoit, J.P., 2006. 99mTc/188Re-labelled lipid nanocapsules as promising radiotracers for imaging and therapy: formulation and biodistribution. Eur. J. Nucl. Med. Mol. Imaging 33, 602–607.

Barone, M., Ettorre, G.C., Ladisa, R., Schiavariello, M., Santoro, C., Francioso, G., Vinciguerra, V., Francavilla, A., 2003. Transcatheter arterial chemoembolization (TACE) in treatment of hepatocellular carcinoma. Hepatogastroenterology 50, 183–187.

Bralet, M.P., Pichard, V., Ferry, N., 2002. Demonstration of direct lineage between hepatocytes and hepatocellular carcinoma in diethylnitrosamine-treated rats. Hepatology 36, 623–630.

Breedis, C., Young, G., 1954. The blood supply of neoplasms in the liver. Am. J. Pathol. 30, 969–977.

Cahouet, A., Denizot, B., Hindre, F., Passirani, C., Heurtault, B., Moreau, M., Le Jeune, J., Benoit, J., 2002. Biodistribution of dual radiolabeled lipidic nanocapsules in the rat using scintigraphy and gamma counting. Int. J. Pharm. 242, 367–371.

Clark, H.P., Carson, W.F., Kavanagh, P.V., Ho, C.P., Shen, P., Zagoria, R.J., 2005. Staging and current treatment of hepatocellular carcinoma. Radiographics 25, S3–S23.

Faivre, J., Clerc, J., Gerolami, R., Herve, J., Longuet, M., Liu, B., Roux, J., Moal, F., Perricaudet, M., Brechot, C., 2004. Long-term radioiodine retention and regression of liver cancer after sodium iodide symporter gene transfer in Wistar rats. Cancer Res. 64, 8045–8051.

Forner, A., Hessheimer, A.J., Isabel Real, M., Bruix, J., 2006. Treatment of hepatocellular carcinoma. Crit. Rev. Oncol. Hematol. 60, 89–98.

Gelderblom, H., Verweij, J., Nooter, K., Sparreboom, A., 2001. Cremophor EL: the drawbacks and advantages of vehicle selection for drug formulation. Eur. J. Cancer 37, 1590–1598.

Gerolami, R., Cardoso, J., Bralet, M.P., Cuenod, C.A., Clement, O., Tran, P.L., Brechot, C., 1998. Enhanced in vivo adenovirus-mediated gene transfer to rat hepatocarcinomas by selective administration into the hepatic artery. Gene Ther. 5, 896–904.

Gibaud, S., Demoy, M., Andreux, J.P., Weingarten, C., Gouritin, B., Couvreur, P., 1996. Cells involved in the capture of nanoparticles in hematopoietic organs. J. Pharm. Sci. 85, 944–950.

Heurtault, B., Saulnier, P., Pech, B., Proust, J.E., Benoit, J.P., 2002. A novel phase inversion-based process for the preparation of lipid nanocarriers. Pharm. Res. 19, 875–880.

Heurtault, B., Saulnier, P., Pech, B., Venier-Julienne, M.C., Proust, J.E., Phan-Tan-Luu, R., Benoit, J.P., 2003. The influence of lipid nanocapsule composition on their size distribution. Eur. J. Pharm. Sci. 18, 55–61.

Kawashima, Y., 2001. Nanoparticulate systems for improved drug delivery. Adv. Drug Deliv. Rev. 47, 1–2.

Lacoeuille, F., Garcion, E., Benoit, J.P., Lamprecht, A., in press. Lipid nanocapsules for intracellular drug delivery of anticancer drugs. J. Nanosci. Nanotechnol.

Lamprecht, A., Benoit, J.P., 2006. Etoposide nanocarriers suppress glioma cell growth by intracellular drug delivery and simultaneous P-glycoprotein inhibition. J. Control. Release 112, 208–213.

Le Couteur, D.G., Fraser, R., Cogger, V.C., Mclean, A.J., 2002. Hepatic pseudocapillarisation and atherosclerosis in ageing. Lancet 359, 1612–1615.

Maeda, H., Wu, J., Sawa, T., Matsumura, Y., Hori, K., 2000. Tumor vascular permeability and the EPR effect in macromolecular therapeutics: a review. J. Control. Release 65, 271–284.

Moal, F., Aube, C., Roux, J., Croquet, V., Oberti, F., Torrisani, J., 2001. Treatment of hepatocellular carcinoma by octreotide. Hepatology 34, A2011.

Moghimi, S.M., Hunter, A.C., Murray, J.C., 2001. Long-circulating and target-specific nanoparticles: theory to practice. Pharmacol. Rev. 53, 283–318.

Mosqueira, V.C., Legrand, P., Morgat, J.L., Vert, M., Mysiakine, E., Gref, R., Devissaguet, J.P., Barratt, G., 2001. Biodistribution of long-circulating PEG-grafted nanocapsules in mice: effects of PEG chain length and density. Pharm. Res. 18, 1411–1419.

Ng, I.O., Liu, C.L., Fan, S.T., Ng, M., 2000. Expression of P-glycoprotein in hepatocellular carcinoma. A determinant of chemotherapy response. Am. J. Clin. Pathol. 113, 355–363.

Seeff, L.B., 2004. Introduction: the burden of hepatocellular carcinoma. Gastroenterology 127, S1–S4.

Sells, R.A., Owen, R.R., New, R.R., Gilmore, I.T., 1987. Reduction in toxicity of doxorubicin by liposomal entrapment. Lancet 2, 624–625.

Storm, G., Van Gessel, H.J., Steerenberg, P.A., Speth, P.A., Roerdink, F.H., Regts, J., Van Veen, M., De Jong, W.H., 1987. Investigation of the role of mononuclear phagocytes in the transportation of doxoubicin-containing liposomes into a solid tumor. Cancer Drug Deliv. 4, 89–104.

Torchilin, V.P., Trubetskoy, V.S., 1995. Which polymer can make nanoparticulate drug carriers long-circulating? Adv. Drug Deliv. Rev., 141–155.

Vittaz, M., Bazile, D., Spenlehauer, G., Verrecchia, T., Veillard, M., Puisieux, F., Labarre, D., 1996. Effect of PEO surface density on long-circulating PLA-PEO nanoparticles which are very low complement activators. Biomaterials 17, 1575–1581.